Available online at www.sciencedirect.com
ScienceDirect
Trans. Nonferrous Met. Soc. China 22(2012) 2883−2890
Transactions of Nonferrous Metals Society of China
www.tnmsc.cn

Low temperature mechanical properties of as-extruded Mg−10Gd−3Y−0.5Zr magnesium alloy

ZHANG Xue-feng[1], WU Guo-hua[1], LIU Wen-cai[1], DING Wen-jiang[1, 2]

1. National Engineering Research Center of Light Alloy Net Forming, Shanghai Jiao Tong University, Shanghai 200240, China;
2. State Key Laboratory of Metal Matrix Composite, Shanghai Jiao Tong University, Shanghai 200240, China

Received 8 October 2011; accepted 13 March 2012

Abstract: Influence of multi-cycle cryogenic treatment and tensile temperature on microstructure, mechanical properties and fracture mechanism of as-extruded Mg−10Gd−3Y−0.5Zr magnesium alloy was investigated. The results show that there have no significant changes in tensile properties of the tested alloy after 10 d in liquid nitrogen immersion or 10 cycles of high-low temperature treatment at all test temperatures. The room temperature ultimate tensile strength increases from 398 MPa to 417 MPa after 20 cycles of high-low temperature treatments. Compared with the room temperature, the tested alloys exhibit higher tensile properties at low temperatures. At −196 °C, the yield strength and ultimate tensile strength of the as-extruded-T5 Mg−10Gd−3Y−0.5Zr alloy are 349 MPa and 506 MPa, respectively, increasing by about 18% and 27%, respectively. The transgranular cleavage fracture mechanism is observed at room temperature, while at low temperatures both ductile fracture and cleavage fracture behaviors coexist.
Key words: magnesium alloy; Mg−10Gd−3Y−0.5Zr alloy; heat treatment; mechanical property; super-low temperature

1 Introduction

Magnesium alloys have been increasingly applied to structural components in the automotive and aerospace industries to reduce fuel consumption and greenhouse gas emissions with excellent properties such as low density, high specific strength, high damping capacity, and good recyclability [1−3]. It has been demonstrated that rare earth metals (RE) are the most effective elements to improve the mechanical properties of magnesium especially [4−6]. The strength of these Mg−RE alloys is achieved essentially via precipitation hardening [7−9], which is higher than that of conventional Al and Mg alloys. Among them, the Mg−Gd−Y recently developed magnesium alloys exhibit higher strength and better plasticity compared with the other Mg−RE alloy. Many investigations related to the microstructure and mechanical properties of the Mg−Gd−Y system have been reported [10−13]. Given the results in these literatures, the Mg−10Gd−3Y−0.5Zr alloy exhibits higher strength and better plasticity compared with the other Mg−Gd−Y alloy. With regard to the excellent mechanical properties, the Mg−10Gd−3Y−0.5Zr alloys will have a good prospect in aerospace industry as lunar spacecraft. It should be noted that the aerospace materials used for working in the space environment will have to withstand the combined actions of particle irradiation, electromagnetic interference and the great temperature gap.

However, the amount of information available on the super-low temperature mechanical properties of the Mg−10Gd−3Y−0.5Zr alloy remains quite scarce to date. In order to expand the applications of this system, it is necessary to investigate the super-low temperature mechanical properties of the alloy. Therefore, in this work, the harsh lunar temperature environment was simulated by long time liquid nitrogen soaking and multi-cycle high-low temperature treatments, the effects of multi-cycle cryogenic treatment and tensile

Foundation item: Project (51275295) supported by the National Natural Science Foundation of China; Project (USCAST2012-15) supported by the Funded Projects of SAST-SJTU Aerospace Advanced Technology Joint Research Centre, China; Project (20120073120011) supported by the Research Fund for the Doctoral Program of Higher Education of China
Corresponding author: WU Guo-hua; Tel: +86-21-54742630; E-mail: ghwu@sjtu.edu.cn
DOI: 10.1016/S1003-6326(11)61546-X

temperature on microstructure, mechanical properties and fracture mechanism of the as-extruded Mg−10Gd−3Y−0.5Zr alloy were investigated.

2 Experimental

The magnesium alloy Mg−10Gd−3Y−0.5Zr (nominal composition in mass fraction, %: 10 Gd, 3 Y, 0.5 Zr, balance Mg) used in this work was prepared from industrial pure magnesium (purity>99.95%) and three master alloys Mg−25Gd, Mg−25Y and Mg−30Zr alloys in an electric resistance furnace under the mixed atmosphere of CO_2 and SF_6 with the volume ratio of 100:1, and cast in steel mould of *d*100 mm×200 mm. The real chemical composition was determined to be Mg−9.86Gd−2.84Y−0.43Zr by an inductively coupled plasma analyzer (Perkin Elmer, Plasma−400). Before extruding, the cast ingots were firstly homogenized at 500 °C for 10 h in an electric furnace, then hot-extruded to a cylindrical bar of 20 mm in diameter at the extrusion speed of 12 mm/s after soaking at 450 °C for 2 h, with an extrusion ratio of 25.

The cryogenic soaking treatment and multi-cycle high-low temperature treatment were applied to some of the as-extruded cylindrical bars after peak aging treatment at 225 °C for 10 h. Considering the large temperature difference between day and night on lunar surface (150−180 °C) and cost experiment, the lunar-environment temperature was simulated in liquid nitrogen and oil bath. A high-low temperature process was defined as follows: the as-extruded and aged bars were firstly immersed in liquid nitrogen with −196 °C for 11 h, followed natural aging at room temperature for 2 h, and then treated by artificial aging in oil bath furnace at 200 °C for 11 h. As described above, peak aging treatment (T5, 225 °C, 10 h), T5 aging treatment (225 °C, 10 h) followed by 10 d (10D) cryogenic soaking treatment at −196 °C, T5 aging treatment (225 °C, 10 h) followed by 10 cycles (10C) of high-low temperature treatment, and T5 aging treatment (225 °C, 10 h) followed by 20 cycles (20C) of high-low temperature treatment were applied to four as-extruded bars, respectively. And the four condition alloys studied hereinafter can be simply designated as extruded-T5-10D, extruded-T5-10C, extruded-T5-20C and extruded-T5, respectively, as shown in Table 1.

Specimens for mechanical testing were machined with the load axis parallel to extrusion direction (ED) for the as-extruded bars. Tensile properties of the four alloys were determined using sheet specimens with the marked dimensions of 15 mm in gauge length, 3.6 mm in width and 2 mm in thickness on the Zwick/Roell Z020 tensile testing machine at room temperature and on MTS-SANS CMT5000 separately at low temperatures. The initial strain rate was 1.67×10^{-5} s^{-1}. Vickers hardness testing was taken using 49 N of load and holding time of 30 s. Phase composition was characterized by X-ray diffraction (XRD) using Ni-filtered Cu K_α radiation. The microstructures, chemical composition analysis and tensile fracture surfaces of the investigated alloys were observed respectively by using optical microscope (OM, XJL−03) and scanning electron microscope (SEM, JSM−7600F), respectively.

Table 1 Heat treatment conditions for tested alloy

Alloy	Treatment condition
Extruded-T5-10D	(225 °C, 10 h)+(−196 °C, 10 d)
Extruded-T5-10C	(225 °C, 10 h)+ (−196 °C, 200 °C, 10 cycles)
Extruded-T5-20C	(225 °C, 10 h)+ (−196 °C, 200 °C, 20 cycles)
Extruded-T5	As-received

3 Results

3.1 Microstructures of Mg−10Gd−3Y−0.5Zr alloys at room temperature

Figure 1 shows the optical microstructure of the as-cast Mg−10Gd−3Y−0.5Zr alloy. It is clear that significant quantities of the eutectic phases decorate the grain boundaries and triple points. The microstructures of the as-extruded Mg−10Gd−3Y−0.5Zr alloys under different conditions at room temperature are shown in Fig. 2. As seen from Fig. 2, the microstructures of the four alloys mainly consist of banded microstructures that are typical characteristic of deformation structure. The eutectic compounds have almost dissolved completely into the matrix, the remnant eutectic phase in the as-cast alloy is broken into small particles, which distribute as streamline along the extrusion direction [14−16]. As seen from Fig. 2(c), the grain refinement in α-Mg matrix can be observed obviously and the grain size in the organization is more even, which can lead to the improvement of both strength and plasticity.

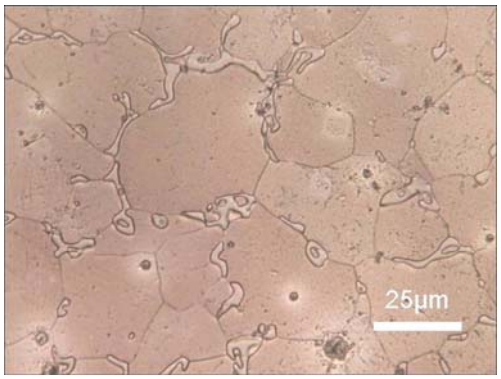

Fig. 1 Optical microstructure of as-cast Mg−10Gd−3Y−0.5Zr alloy

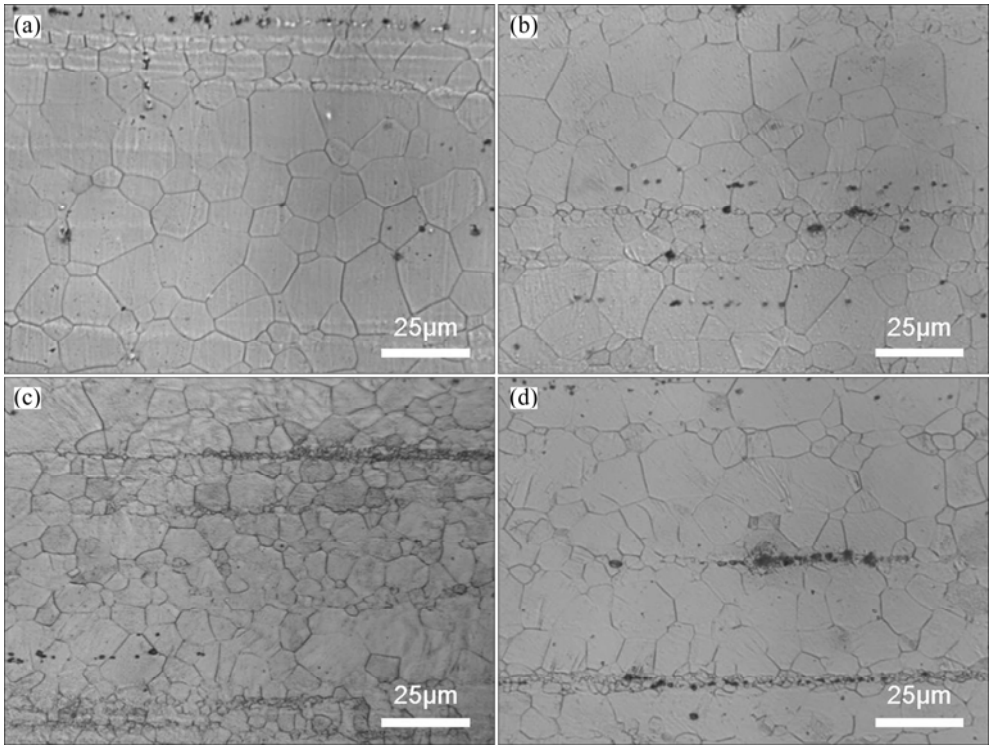

Fig. 2 Optical microstructures of as-extruded alloys at room temperature under different conditions: (a) Extruded-T5-10D; (b) Extruded-T5-10C; (c) Extruded-T5-20C; (d) Extruded-T5

Figures 3 and 4 show the XRD pattern and EDX analysis results of the extruded-T5 alloy, respectively. It can be observed that the extruded-T5 alloy is mainly composed of α-Mg, $Mg_{24}(Gd,Y)_5$ and Mg_5Y precipitates [17]. Meanwhile, no significant changes can be found according to the XRD patterns under different conditions.

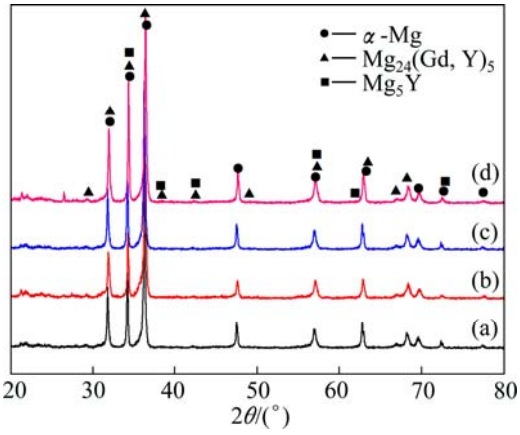

Fig. 3 XRD patterns of as-extruded alloys under different conditions: (a) Extruded-T5-10D; (b) Extruded-T5-10C; (c) Extruded-T5-20C; (d) Extruded-T5

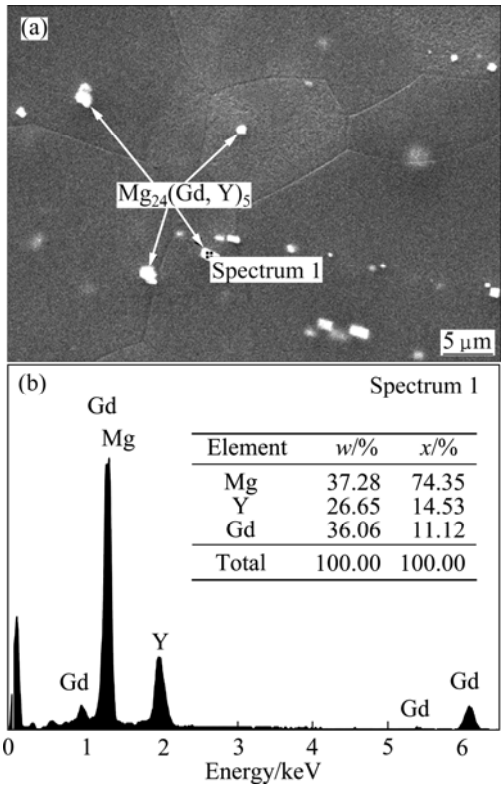

Fig. 4 SEM image (a) and corresponding EDS result (b) of extruded-T5 alloy

3.2 Tensile properties at room temperature

The tensile properties and hardness of the Mg−10Gd−3Y−0.5Zr alloy under different conditions at room temperature are shown in Fig. 5 and Table 2. As seen from Fig. 5 and Table 2, the yield strength (YS), ultimate tensile strength (UTS) and elongation (EL) of

the extruded-T5 alloy are 295MPa, 398MPa and 5.2%, respectively. After 10 cycles of high-low temperature treatment (extruded-T5-10C), there are no significant changes in the YS and UTS compared with extruded-T5 alloy, while the elongation decreases slightly from 5.2% to 3.1%. However, 20 cycles of high-low temperature treatment (extruded-T5-20C) can improve the tensile properties of the extruded-T5 alloy, i.e., the UTS and elongation increase from 398 MPa and 5.2% to 417 MPa and 8.4%, respectively, which can be explained by the grain refinement strengthening according to Fig. 2(c).

No obvious difference in strength and elongation can be found in Table 2. After 10 d of liquid nitrogen soaking, extruded-T5-10D alloy shows the mechanical properties of YS=291 MPa, UTS=392 MPa and EL=3.5%.

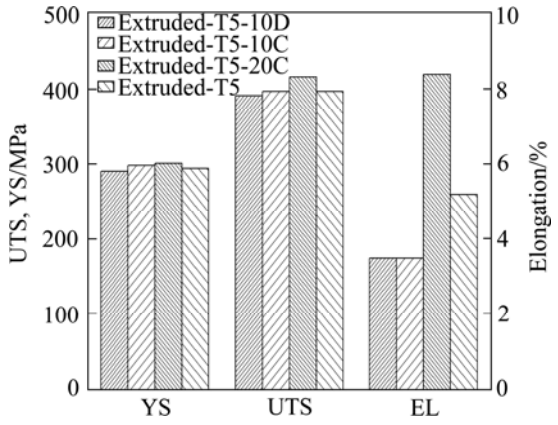

Fig. 5 Tensile results of as-extruded alloys at room temperature under different conditions

Table 2 Tensile properties and hardness of as-extruded alloys at room temperature

Alloy	YS/MPa		UTS/MPa		EL/%		Hardness, Hv	
	Mean	STD	Mean	STD	Mean	STD	Mean	STD
Extruded-T5-10D	291	7.7	392	8.1	3.5	0.3	116	0.7
Extruded-T5-10C	299	6.6	398	9.7	3.1	1.5	118	0.6
Extruded-T5-20C	302	3.6	417	5.7	8.4	1.1	115	0.8
Extruded-T5	295	8.3	398	9.4	5.2	0.9	117	0.7

STD refers to standard deviation from mean value.

3.3 Tensile properties at low temperature

The tensile results of the Mg−10Gd−3Y−0.5Zr alloys under four conditions at low temperature (−196 °C) are shown in Figs. 6 and Table 3. As seen from Table 3, compared with the room temperature, the tested alloys exhibit higher tensile properties at low temperatures. The YS and UTS of the extruded-T5 alloy are 349 MPa and 506 MPa, respectively. Compared with room temperature (25 °C), the improvement of about 18% and 27% has been achieved respectively. Meanwhile, the elongation of the extruded-T5 alloy also increases from 5.2% to 7.1%.

The YS and UTS of the extruded-T5-10D alloy tested at −196 °C are 381 MPa and 490 MPa, respectively. Similarly, obvious improvements in tensile strength of the extruded-T5-10C and extruded-T5-20C alloys are also achieved at low tensile temperatures. Moreover, as seen from Fig. 6, the improvement of tensile properties induced by low temperature or high-low temperature cycle treatments at −196 °C can also be found. Compared with room temperature, the extruded-T5-10C alloy exhibits higher tensile properties at −196 °C as YS=384 MPa and UTS=516 MPa.

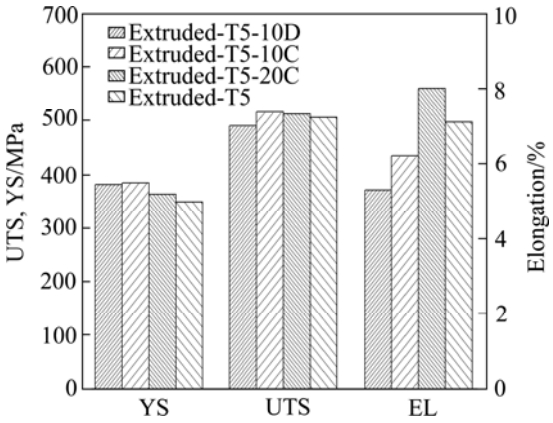

Fig. 6 Tensile results of as-extruded alloys at −196 °C under different conditions

Table 3 Tensile properties of as-extruded alloys at −196 °C

Alloy	YS/MPa		UTS/MPa		EL/%	
	Mean	STD	Mean	STD	Mean	STD
Extruded-T5-10D	381	7.3	490	8.6	5.3	1.3
Extruded-T5-10C	384	8.7	516	9.5	6.2	1.2
Extruded-T5-20C	363	7.9	512	8.1	8.0	0.5
Extruded-T5	349	7.6	506	9.2	7.1	1.3

3.4 Fractography

Figure 7 shows the optical microstructures of ruptured samples of the extruded-T5 and extruded-T5-10C alloys perpendicular to the fracture surface which deformed at different tensile temperatures (25 °C and −196 °C). As seen from Fig. 7, secondary cracks and the twinning near the fracture surface are observed in extruded-T5 alloy, while little secondary cracks can be found in the extruded-T5-10C alloy.

For the extruded-T5 alloy tested at room temperature (Fig. 7(a)), some of the secondary microcracks locate inside the grains and some distribute along the residual eutectics at grain boundaries. Extensive twinning is also found inside the grains. At −196 °C in Fig. 7(b), it can be noticed clearly that the number of twinning in the matrix is less than that at 25

°C, and the majority of the twinning exists in the interior of the large size grain. The secondary microcracks were also observed, most of which completely stuck in the grain interior.

As seen from Figs. 7(c) and (d), no obvious secondary microcracks can be found in the extruded-T5-10C alloy at both room and low temperatures. However, twinning can still be observed. And similarly, the number of the twinning in the extruded-T5-10C alloy at −196 °C is smaller than that at room temperature.

The fracture surfaces of tensile specimens of the extruded-T5 and extruded-T5-10C alloys tested at 25 °C and −196 °C are shown in Fig. 8. As seen from Figs. 8(a)

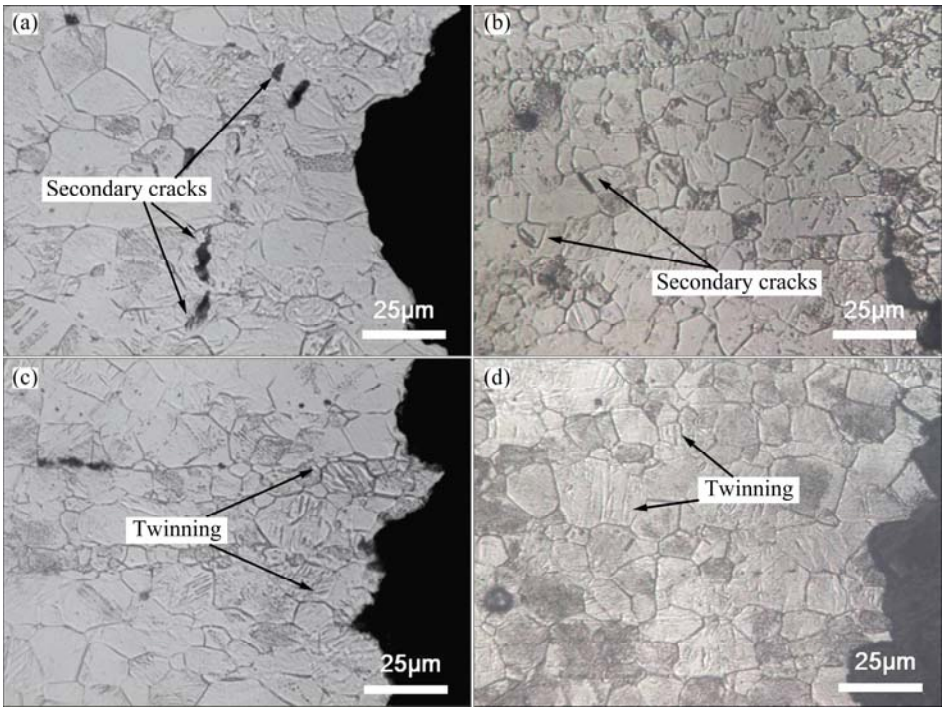

Fig. 7 Optical images of longitudinal section of fracture surfaces of extruded-T5 and extruded-T5-10C alloys tested at different temperatures: (a) Extruded-T5, 25 °C; (b) Extruded-T5, −196 °C; (c) Extruded-T5-10C, 25 °C; (d) Extruded-T5-10C, −196 °C

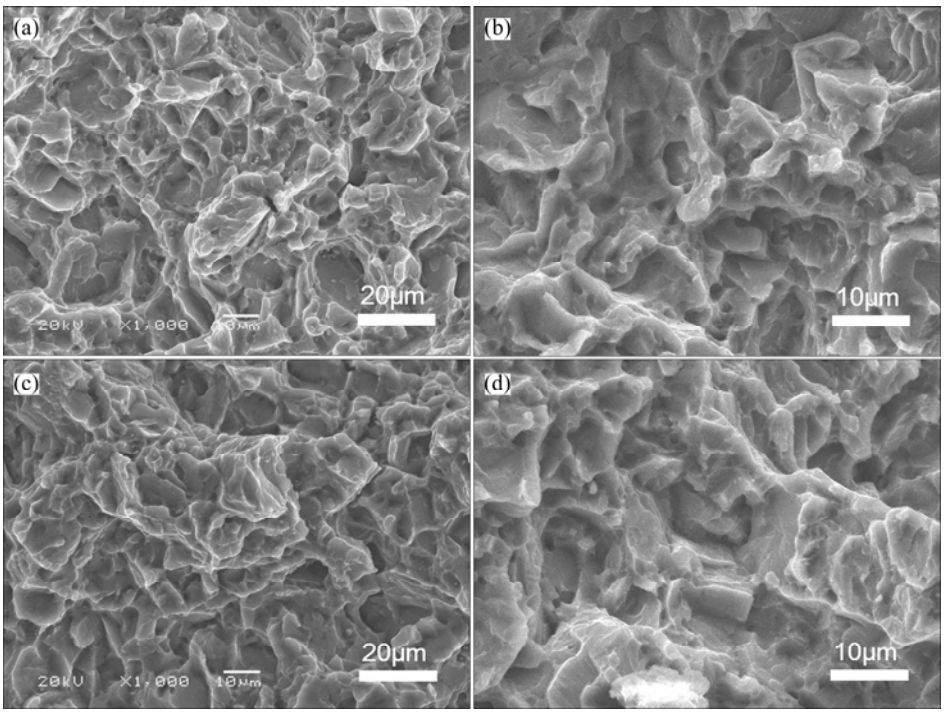

Fig. 8 Typical SEM images showing fracture surfaces of tensile samples of extruded-T5 and extruded-T5-10C alloys tested at different temperatures: (a) Extruded-T5, 25 °C; (b) Extruded-T5, −196 °C; (c) Extruded-T5-10C, 25 °C; (d) Extruded-T5-10C, −196 °C

and (c), the tensile fracture surfaces are mainly composed of cleavage planes, some tearing ridges and fine ductile dimples. But no cleavages in large scale are discovered, indicating that small grains are solely responsible for high strength of the tested alloy at room temperature. The fracture mode of the alloy at room temperature is quasi-cleavage. As seen from Figs. 8(b) and (d) at −196 °C, the number and size of the cleavage planes both decrease. And the shallow dimples with white irregular shape particles inside can be observed on the fracture surface, indicating that crack may initiate from the broken particles and propagate by coalescence of dimples. The fracture surface exhibits more obvious ductile fracture characteristics. According to Fig. 8, it can be seen that the 10 cycles of high-low temperature treatments exhibit little effect on the alloy fracture surfaces at both room and low temperatures.

4 Discussion

4.1 Effect of thermal cycle on tensile properties of tested alloy

The high-low temperature cycle treatment has greater effects on the mechanical properties of the extruded-T5 alloys at low temperatures compared with room temperature. According to Fig. 6 and Table 3, the tensile properties firstly increase after 10 cycles, and then slightly decrease after another 10 cycles treatment.

According to Refs. [9,18,19], with the increase of aging time, the precipitation sequence of the Mg−Gd−Y−Zr alloy during isothermal ageing at 225 °C consists of the following steps: α-Mg supersaturated solid solution (S.S.S.S.)→metastable β'' ($D0_{19}$)→ metastable β' (cbco)→metastable β_1 (FCC)→stable β (FCC). Therefore, the high-low (−196 °C−200 °C) temperature cycle may have significant effects on the type, quantity and distribution characteristics of aging precipitates, which further affect the tensile properties of the alloy. And the aging precipitate behavior of the Mg−Gd−Y−Zr alloy can be considered as the diffusion process of rare-earth atoms (Gd, Y) in the matrix. According to the TEM results in Ref. [20], as seen from Fig. 9, there exists the diffraction spot of β'' besides that of β' in the SAED pattern of the Mg−Gd−Y−Zr alloy after 4 high-low temperature (−196 °C, 12 h+200 °C, 12 h) cycles, which strengthen the alloy. Based on this conclusion and the ageing sequence of the Mg−Gd−Y−Zr alloy above, with the increase of the high-low temperature cycle, the β'' will transform into β' phase. However, with further increasing the high-low temperature cycle treatment, the β_1 phase appears via an in situ transformation from the decomposed β' phase, although it grows in a direction that is different from that of the previous β' phase growth. Comparatively, the strengthening effect of the β' phase on mechanical properties at the peak-aging stage is higher than that of the β and β_1 phases at the under-aging and over-aging stages. And the improvement of tensile properties of the extruded-T5-10C alloy can be attributed to the increase of β'.

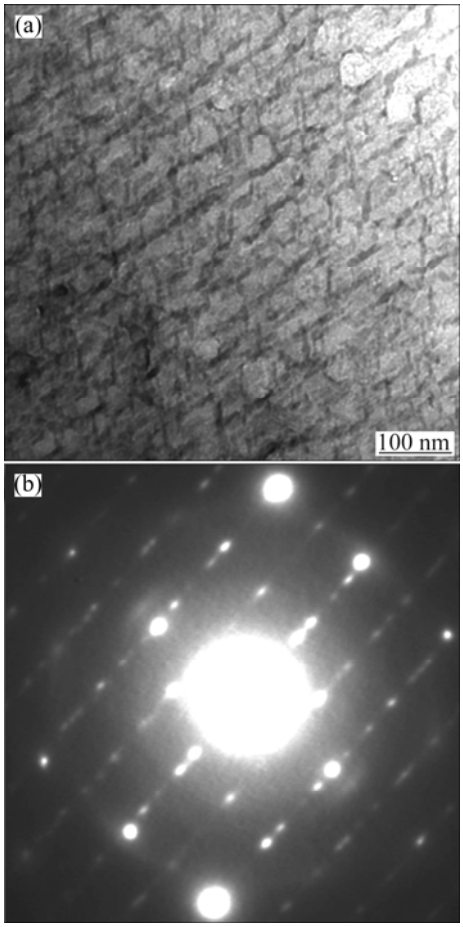

Fig. 9 TEM image and SAED pattern of sample treated by (−196 °C, 12 h+200 °C, 12 h) regime 4 times: (a) TEM image; (b) SAED pattern (B// $[01\bar{1}2]$) [20]

However, the phase transformations in the high-low temperature cycle almost have no effect on the tensile properties of alloys at room temperature. The reasons and mechanisms for this phenomenon still depend on further studies. But the obvious changes in the tensile strength of the extruded-T5-20C alloy can be explained as follows. As well known, at low temperatures, the thermal vibration energies of atoms decrease greatly and increased forces are required for dislocations to move across the barrier. And there also come into being internal stress and increasing internal energy in the matrix under the low temperature condition. It can result in small subgrain structures and further refine the grains locally, which can be observed in Fig. 2(c). The grain refinement in α-Mg matrix can be used to explain the

relative improvement of tensile properties of the extruded-T5-20C alloy at room temperature compared with extruded-T5 alloy.

4.2 Effect of tensile temperature on fracture mechanism

Magnesium alloy has different deformation mechanisms at different temperatures, leading to different fracture mechanisms. Magnesium has an asymmetric hexagonal close-packed (HCP) structure. Twinning is an especially important deformation mechanism for HCP magnesium alloy at room temperature. At room temperature, slip deformation in magnesium mainly depends on $\{0001\}\langle 11\bar{2}0\rangle$ which can only provide two independent slip systems, while at least five independent slip systems are required for every grain deformation in polycrystalline. This law further forces $\{10\bar{1}2\}\langle 10\bar{1}1\rangle$ to contribute to deformation by twinning [21].

Based on the microstructural analysis and tensile results, it can be known that there are no obvious necking and elongation in fracture microstructures at 25 °C. A large amount of twinning can be observed. Twin deformation causes the rapid expansion of cracks, exhibiting poor plasticity. Compared with the extruded-T5-10C alloy, more extensive secondary microcracks can be observed in extruded-T5-10C alloy at room temperature. The rapid expansion of cracks inside the grain results in large smooth cleavage planes, making the grain surfaces consist of several smooth cleavage planes. The fracture mechanism of the as-extruded alloy tested at room temperature is transgranular cleavage fracture. At −196 °C, less twinning can be found in matrix, and the majority of twins exist in larger size grains. Correspondingly, the secondary microcracks at −196 °C decrease greatly and even disappear. Some irregularly shaped rare-earth particles cause stress concentration to initiate cracks, which propagate and further lead to the formation of microvoids. These microvoids accumulate together continually to form shallow flat dimples, as shown in the SEM images, which display typical ductile fracture characteristics. In addition, some cleavage planes can also be observed from the SEM morphologies, exhibiting cleavage fracture characteristics. Therefore, the fracture mechanism for the as-extruded alloy at −196 °C is mixed ductile fracture and cleavage fracture.

Plasticity of Mg−Gd−Y−Zr alloys at low temperatures was studied by XRD and TEM [22], and the results show that adding Gd and Y elements into Mg make the value of lattice constant c/a decrease to 1.6148, and cryogenic treatment can further reduce it to 1.6113. The c/a value of the Mg−10Gd−3Y−0.5Zr alloy at −196 °C will be smaller than 1.6113, while the decrease of c/a value will lower the critical shear stress of cylinder slip systems and make the alloy enter into multi-system slip at low temperatures. According to Fig. 7, the number of twinning in the matrix is indeed less than that at room temperature, indicating new slip systems initiate at −196 °C rather than through twin deformation. Thus, alloy plasticity gets improved and the fracture mechanism transforms from the original brittle cleavage fracture gradually to ductile fracture, exhibiting mixed fracture mechanism at −196 °C.

5 Conclusions

1) The extruded-T5 Mg−10Gd−3Y−0.5Zr alloy shows the tensile properties at room temperature: YS=295 MPa, UTS=398 MPa and EL=5.2%. After 10 d liquid nitrogen soaking or 10 cycles of high-low temperature treatment, the tensile properties remain almost unchanged. Yet after 20 cycles, the YS is 302 MPa, the UTS increase to 417 MPa, and elongation increases from 5.2% to 8.4%, which can mainly be attributed to the grain refinement.

2) The extruded-T5 Mg−10Gd−3Y−0.5Zr alloy exhibits excellent tensile properties at −196 °C. The YS and UTS reach 349 MPa and 506 MPa respectively, and the elongation reaches 7.1%. The outstanding mechanical properties can be attributed to the increase of the CRSS for dislocation slip and the initiation of new slip systems at low temperatures. Compared with the extruded-T5 alloy, the tensile properties improvement of the extruded-T5-10C alloy can be attributed to the increase of β'.

3) The fracture mechanism at room temperature is transgranular cleavage fracture, while the fracture mechanism is mixed ductile and cleavage fracture at −196 °C.

References

[1] MORDIKE B L, EBERT T. Magnesium: Properties—applications −potential [J]. Materials Science and Engineering A, 2001, 302(1): 37−45.

[2] MORDIKE B L. Creep-resistant magnesium alloys [J]. Materials Science and Engineering A, 2002, 324(1−2): 103−112.

[3] ROKHLIN L L. Magnesium alloys containing rare earth metals: Structure and properties [M]. London: Taylor & Francis, 2003: 1−2.

[4] MOHRI T, MABUCHI M, SATIO N, NAKAMURA M. Microstructure and mechanical properties of a Mg−4Y−3RE alloy processed by thermo-mechanical treatment [J]. Materials Science and Engineering A, 1998, 257(2): 287−294.

[5] NIE Jian-feng, MUDDLE B C. Precipitation in magnesium alloy WE54 during isothermal ageing at 250 °C [J]. Scripta Materialia, 1999, 40(10): 1089−1094.

[6] LI Zhi-cheng, ZHANG Hong, LIU Lu, XU Yong-bo. Growth and morphology of β phase in an Mg−Y−Nd alloy [J]. Materials Letters, 2004, 58(24): 3021−3024.

[7] HONMA T, OHKUBO T, KAMADO S, HONO K. Effect of Zn

additions on the age-hardening of Mg−2.0Gd−1.2Y−0.2Zr alloys [J]. Acta Materialia, 2007, 55(12): 4137−4150.

[8] CHANG Jian-wei, GUO Xing-wu, HE Shang-ming, FU Peng-huai, PENG Li-ming, DING Wen-jiang. Investigation of the corrosion for Mg−*x*Gd−3Y−0.4Zr (*x*=6%, 8%, 10%, 12%, mass fraction) alloys in a peak-aged condition [J]. Corrosion Science, 2008, 50(1): 166−177.

[9] WANG Jun, MENG Jian, ZHANG De-ping, TANG Ding-xiang. Effect of Y for enhanced age hardening response and mechanical properties of Mg−Gd−Y−Zr alloys [J]. Materials Science and Engineering A, 2007, 456(1−2): 78−84.

[10] ANYANWU I A, KAMADO S, KOJIMA Y. Aging characteristics and high temperature tensile properties of Mg−Gd−Y−Zr alloys [J]. Materials Transactions, 2001, 42(7): 1206−1211.

[11] HE Shang-ming, ZENG Xiao-qin, PENG Li-ming, GAO Xiang, NIE Jian-feng, DING Wen-jiang. Precipitation in a Mg−10Gd−3Y−0.4Zr (wt. %) alloy during isothermal aging at 250 °C [J]. Journal of Alloys and Compounds, 2006, 421(1−2): 309−313.

[12] ANYANWU I A, KAMADO S, KOJIMA Y. Creep properties of Mg−Gd−Y−Zr alloys [J]. Materials Transactions, 2001, 42(7): 1212−1218.

[13] HE Shang-ming, ZENG Xiao-qin, PENG Li-ming, GAO Xiang, NIE Jian-feng, DING Wen-jiang. Precipitation in a Mg−10Gd−3Y−0.4Zr (wt. %) alloy during isothermal aging at 250 °C [J]. Journal of Alloys and Compounds, 2006, 421(1−2): 309−313.

[14] ZHANG Xin-min, XIAO Yang, CHEN Jian-mei, JIANG Hao. Influence of extrusion temperature on microstructures and mechanical properties of Mg−9Gd−4Y−0.6Zr alloy [J]. The Chinese Journal of Nonferrous Metals, 2006, 16(3): 518−523. (in Chinese)

[15] HE Shang-ming. Study on the microstructural evolution, properties and fracture behavior of Mg−Gd−Y−Zr(−Ca) alloys [D]. Shanghai: Shanghai Jiao Tong University, 2007. (in Chinese)

[16] HE Shang-ming, ZENG Xiao-qin, PENG Li-ming, GAO Xiang, NIE Jian-feng, DING Wen-jiang. Microstructure and strengthening mechanism of high strength Mg−10Gd−2Y−0.5Zr alloy [J]. Journal of Alloys and Compounds, 2007, 427(1−2): 316−323.

[17] LIU Wen-cai, DONG Jie, SONG Xu, BELNOUE J P, HOFMANN F, DING Wen-jiang, KORSUNSKY A M. Effect of microstructures and texture development on tensile properties of Mg–10Gd–3Y alloy [J]. Materials Science and Engineering A, 2011, 528(6): 2250−2258.

[18] HE Shang-ming, ZENG Xiao-qin, PENG Li-ming, GAO Xiang, NIE Jian-feng, DING Wen-jiang. Precipitation in a Mg−10Gd−3Y−0.4Zr (wt. %) alloy during isothermal aging at 250 °C [J]. Journal of Alloys and Compounds, 2006, 421(1−2): 309−313.

[19] XU Zhou, ZHAO Lian-cheng. Metal solid phase transition theory [M]. Beijing: Science Press, 2004: 13−14. (in Chinese)

[20] TANG Chang-ping, ZHANG Xin-ming, DENG Yun-lai, LI Li, ZHAO Feng-jin, XU Li, ZHANG Guo-yi. Effects of high-low temperature cycle on microstructures and mechanical properties of EW94 magnesium alloy [J]. The Chinese Journal of Nonferrous Metals, 2011, 21(3): 505−512. (in Chinese)

[21] HU Geng-xiang, CAI Xun. Fundamentals of materials science [M]. Shanghai: Shanghai Jiao Tong University Press, 2000. (in Chinese)

[22] XIAO Yang, ZHANG Xin-ming. Low temperature plastic analysis of Mg−9Gd−4Y−0.6Zr alloy [J]. Special Casting & Nonferrous Alloys, 2010, 30(9): 794−796. (in Chinese)

挤压态 Mg−10Gd−3Y−0.5Zr 镁合金的低温力学性能

张学锋[1], 吴国华[1], 刘文才[1], 丁文江[1,2]

1. 上海交通大学 轻合金精密成型国家工程研究中心，上海 200240；
2. 上海交通大学 金属基复合材料国家重点实验室，上海 200240

摘 要：研究多循环低温交变(液氮浸泡处理)和拉伸温度对挤压态 Mg−10Gd−3Y−0.5Zr 镁合金的微观组织、力学性能以及断裂机制的影响。结果表明，Mg−10Gd−3Y−0.5Zr 合金经 10 d 液氮浸泡或 10 个周期高低温交变循环后，合金室温力学性能基本不变；而经过 20 个周期高低温循环后，合金的室温抗拉强度由 398 MPa 升高到 417 MPa。在−196 °C 下拉伸时，挤压态 Mg−10Gd−3Y−0.5Zr 镁合金的屈服强度和抗拉强度均大幅度提高，分别为 349 MPa 和 506 MPa，分别增长了 18%和 27%。合金室温断裂机制为穿晶解理断裂，而低温条件下为韧性断裂和解理断裂并存的混合断裂机制。

关键词：镁合金；Mg−10Gd−3Y−0.5Zr 合金；热处理；力学性能；超低温

(Edited by LI Xiang-qun)